



Nafion[®] nanocomposite membranes: Effect of fluorosurfactants on hydrophobic silica nanoparticle dispersion and direct methanol fuel cell performance

Chi Hoon Park, Hong Keon Kim, Chang Hyun Lee, Ho Bum Park^{**}, Young Moo Lee^{*}

School of Chemical Engineering, Hanyang University, Seoul 133-791, Republic of Korea

ARTICLE INFO

Article history:

Received 6 February 2009

Received in revised form 21 May 2009

Accepted 8 June 2009

Available online 24 June 2009

Keywords:

Polymer electrolyte membrane

Nanocomposite

Fluorosurfactant

Nanoparticle

Direct methanol fuel cell

ABSTRACT

Nafion[®]-silica nanocomposite membranes are successfully prepared by adding hydrophobic silica nanoparticles to a Nafion[®] solution. To distribute these nanoparticles evenly in the Nafion[®] matrix, various fluorosurfactants of different ionic character are employed. Fluorosurfactants with acid groups such as phosphonic acid and sulfonic acid play an important role in simultaneously increasing the homogeneous dispersion of silica nanoparticles, enhancing proton conductivity, and reducing the methanol permeability of the nanocomposite membranes. Therefore, the dispersion properties of inorganic fillers such as silica can significantly affect nanocomposite performance in direct methanol fuel cell (DMFC) applications, whereas surfactants, if used properly, can improve the nanocomposite membrane properties. In particular, a commercial fluorosurfactant containing a sulfonic acid group (Zonyl[®] TBS) at the end of the surfactant chain exhibits better miscibility with the Nafion[®] ionomer. This feature results in a reduction in the dimensional change of the nanocomposite membrane due to relatively lower water swelling and significantly reduced methanol permeability through the membrane. A membrane-electrode assembly (MEA) prepared from a Nafion[®]-silica nanocomposite membrane with TBS shows the highest DMFC performance in terms of voltage vs. current density ($V-I$) and power density vs. current density ($P-I$). The current densities at 0.4 V and 90 °C are 342, 508, and 538 mA cm⁻² with 1, 3 and 5 M methanol being fed at the anode side, respectively.

© 2009 Elsevier B.V. All rights reserved.

1. Introduction

Numerous scientific and technical approaches to alleviate the emission of greenhouse gases such as carbon dioxide and methane have been investigated due to concerns about global warming. The development of zero-emission power sources is therefore a global priority. Among the candidates for such power sources, proton exchange membrane fuel cells (PEMFCs) are particularly promising for mobile and stationary applications because they are environmentally friendly and have a highly efficient energy-conversion mechanism [1–3]. A direct methanol fuel cell (DMFC) is a type of PEMFC that operates with liquid methanol as the fuel instead of hydrogen. A DMFC offers many advantages as a portable power source in applications such as laptop computers, cellular phones, and personal multimedia players. In a DMFC, electrical energy is generated *via* the electrochemical reaction of methanol and oxygen in air to generate heat, water and carbon dioxide, without any toxic by-products [4]. The theoretical specific energy (ca. 6080 Wh kg⁻¹)

of a DMFC is much higher than the ~200 Wh kg⁻¹ of a rechargeable Li-ion battery [5–7] and thereby ensures a much longer operation time. Despite such benefits, however, efficiency and power density of DMFCs compared with hydrogen-fuelled PEMFCs need to be improved if commercialization is to be realized [4]. In these cells, the oxidation reaction from methanol to hydrogen ions (protons) is slower than in the case of hydrogen. Moreover, there is a large crossover of methanol through the polymer electrolyte membrane that gives rise to a mixed-potential at the cathode side, and this decreases the electrochemical performance of a DMFC [8–10]. To resolve these problems, new polymer electrolyte membranes with low methanol permeability are required.

To date, various approaches have been taken to reduce methanol crossover through polymer electrolyte membranes. Crosslinking and interpenetrating networks have been used to prevent excessive water swelling due to the high degree of sulfonation and thus reduce methanol permeability in highly water-swollen states [11,12]. Methanol permeability can be lowered by tuning the hydrophilic channel size in hydrophilic-hydrophobic block copolymer membranes or by surface modification of polymer electrolyte membranes [13–15]. Organic-inorganic nanocomposite membranes with nanometer size fillers have been explored intensively and remain one of the most interesting avenues for the preparation of electrolytes for application in fuel cells [9,11,16–21].

* Corresponding author. Tel.: +82 2 2220 0525.

** Corresponding author. Tel.: +82 2 2220 2338.

E-mail addresses: badtzhb@hanyang.ac.kr (H.B. Park), ymlee@hanyang.ac.kr (Y.M. Lee).

In a previous studies [21–23], various hydrocarbon-based nonionic surfactants consisting of hydrophobic and hydrophilic segments (e.g., PEO_x-PPO_y-PEO_x triblock copolymers) were used to disperse nanometer-size fillers (such as silica) evenly in hydrocarbon-based polymer electrolyte membranes. Without such surfactants, it was difficult to avoid the formation of large clusters, caused by self-agglomeration of small nanoparticles, that led to poor electrochemical performance, even though hydrophilic surface-treated nanoparticles were employed for improved compatibility [23]. When amphiphilic surfactants were used, however, the polymer electrolyte nanocomposite membranes showed a well-distributed nanostructure and thus an improved fuel cell performance [23].

Recently, organic–inorganic composite membranes based on Nafion® have been produced by the addition of hygroscopic inorganic fillers such as silica, titania, zirconia, mixed silicon–titanium oxides, zeolites, silicon–aluminum oxides, and montmorillonite [9,16,19,24,25]. In the present work, using the same concept, Nafion®-based nanocomposite membranes were prepared because Nafion® is the only commercially available membrane for fuel cells. Nevertheless, current Nafion® membranes cannot completely fulfill the requirements for DMFC applications because methanol is readily transported together with solvated protons by electro-osmotic drag, as well as by diffusion through the water-filled hydrophilic channels within the Nafion® matrix [26].

Therefore, it is the objective of this study to examine the effect of the dispersion properties of nanometer inorganic fillers on the electrochemical performance of single cells which employed Nafion®-based nanocomposite membranes with nanometer inorganic fillers that were intended to reduce the methanol permeability. A further goal is to study the effect of fluorosurfactants on the hydrophobic silica dispersion and on the electrochemical performance of the single cells made with such additions. For this purpose, commercial fluorosurfactants with different ionic characteristics were chosen as dispersants to distribute inorganic nanoparticles within the Nafion® matrix, given their improved compatibility with Nafion®.

2. Experimental

2.1. Preparation of Nafion®–silica nanocomposite membranes

0.5 g of hydrophobic silica (Aerosil 812, Degussa Chemical Co., Düsseldorf, Germany; average particle size = 7 nm, BET surface area = 220 ± 25 m² g⁻¹) and 1.5 g of each fluorosurfactant solution (Zonyl® FSP (FS1) and TBS (FS2), DuPont, USA; see Table 1 for further information) were stirred into 10 g of a mixture of isopropyl alcohol (IPA) and water (3:1 by weight) with sonication for 2 h. Then, 0.96 g of the mixture was added into 20 g of a Nafion® solution (20 wt%) (DE 2021, DuPont, Wilmington, DE, USA). The solution was stirred vigorously at ambient temperature for 12 h and further sonicated for 2 h. After degassing, the solution was cast on a clean glass plate and dried in a vacuum oven at 60 °C for 24 h to obtain transparent Nafion®–silica nanocomposite membranes. These nanocomposite membranes were treated successively with a 1 M NaCl solution for 24 h to avoid probable thermal decomposition of the sulfonic acid groups within Nafion® on further heat treatment. The membranes in sodium salt form were rinsed several times with deionized water and then dried at 80 °C in a vacuum

oven for 6 h. The membranes were thermally treated at 240 °C for 1 h. Then, Nafion®–silica nanocomposite membranes in sodium salt form were transformed into their protonated form by placement in 1 M boiling sulfuric acid for 1 h, followed by successive treatment with deionized water at 100 °C for 1 h to remove excessive sulfuric acid in the membranes. Nafion®–silica nanocomposite membranes without fluorosurfactant and recast Nafion® membranes (control) were also prepared according to the procedure described above.

2.2. Membrane characterization

A titration method was used to measure the ion-exchange capacity (IEC) values of the recast Nafion® and Nafion® nanocomposite membranes prepared in this study. A dry Nafion®–silica nanocomposite film (4 cm × 4 cm) was weighed and then immersed in a 0.01 M NaCl solution for 24 h. After the hydrogen ions were fully released, the solution was titrated with a 0.01 M NaOH solution. The IEC values (meq g⁻¹) were calculated from the volume of the added NaOH solution and the weight of each sample film.

The thermal stabilities of the nanocomposite membranes were measured at a heating rate of 10 °C min⁻¹ in the temperature range from room temperature to 500 °C under an air purge using thermal gravimetric analysis (SDT 2960, TA Instruments, New Castle, DE, USA).

The mechanical properties of the nanocomposite membranes in both dry and hydrated states were measured using a Universal Test Machine (AGS-J, Shimadzu, Kyoto, Japan) and the ASTM D882 method [23]. Each film in the protonated form was strained at a speed of 5 mm min⁻¹. For nanocomposite membranes in a dry state, mechanical properties were measured at room temperature under atmospheric conditions. To keep membranes in a hydrated state, deionized water was sprayed on to membrane specimens during measurement.

For water uptake and x–y dimensional change measurements, membrane samples (4 cm × 4 cm) were dried thoroughly in a vacuum oven at 100 °C for more than 24 h. The weight and length (x–y direction) of the dried membranes were measured. The samples were then immersed in deionized water at different temperatures (30, 60, and 90 °C) overnight. The weight and length of the fully hydrated membranes were then measured immediately after removing excessive water on the surface with tissue paper. The water uptake (%) and dimensional change in the x–y direction (%) were calculated using the following equations:

$$\text{Water uptake (\%)} = \left(\frac{M_{\text{wet}} - M_{\text{dry}}}{M_{\text{dry}}} \right) \times 100 \quad (1)$$

$$\text{Dimensional change (\%)} = \left(\frac{D_{\text{wet}} - D_{\text{dry}}}{D_{\text{dry}}} \right) \times 100 \quad (2)$$

Each membrane dimension was measured using a video microscope system (ICS-305B, Sometech, Seoul, Korea) to minimize errors due to fast desorption of water molecules in the hydrated membranes.

The silica dispersion was observed with a field-emission scanning electron microscope (FE-SEM, JSM-6330F, JEOL, Tokyo, Japan). Before measurement, all membrane samples were thoroughly dried in a vacuum oven for at least 24 h.

Table 1

Physical properties of fluorosurfactants used in this study.

Surfactant	Ionic character	Molecular weight	Density (g mL ⁻¹)	Composition
Zonyl® FSP	Anionic	ca. 600	1.15	[F(CF ₂ CF ₂) ₂ CH ₂ CH ₂ O] _m P(O)(ONH ₄) _n
Zonyl® TBS	Anionic	ca. 500	1.20	F(CF ₂ CF ₂) _x CH ₂ CH ₂ SO ₃ H

l = 1–7; *m* = 1 or 2; *n* = 2 or 1; *x* = 1–9.

The proton conductivity (σ , $S\text{ cm}^{-1}$) of each membrane coupon ($1\text{ cm} \times 4\text{ cm}$) was obtained by applying $\sigma = l/RS$ (l is the distance between reference electrodes and S is the cross-sectional area of the membrane coupon). Ohmic resistance (R) was measured by four-point probe alternating current (ac) impedance spectroscopy using an electrode system connected to an impedance/gain-phase analyzer (Solartron 1260, Farnborough Hampshire, ONR, UK) and an electrochemical interface (Solartron 1287) [27]. Impedance measurements were performed in deionized water at 30, 45, 60, 75, and 90 °C.

A two-chamber diffusion cell was used to measure methanol permeability ($\text{cm}^2\text{ s}^{-1}$). Each chamber was filled with 10 M (34 wt%) methanol at the donor side and deionized water at the receiving side. The methanol concentration in the water chamber was measured every 30 min using a gas chromatograph (GC-14B, Shimadzu, Kyoto, Japan) equipped with a thermal conductivity detector (TCD). The methanol permeability was calculated from the slope of the methanol concentration as a function of time. Each measurement was repeated at least five times to guarantee reproducible results.

2.3. Direct methanol fuel cell test

DMFC performance was tested by measuring the polarization curve of MEAs prepared from Nafion®–silica nanocomposite membranes. For MEA preparation, the catalyst ink for the anode and cathode was prepared using a 5 wt% solution (DE521, specific gravity = 0.92–0.94, total acid capacity = 0.95–1.03, DuPont, USA), Pt/Ru black (Hispec 6000, Johnson Matthey, London, UK) for the anode catalyst, Pt black (Hispec 1000, Johnson Matthey, London, UK) for the cathode, and an IPA/water mixture. The ink was sprayed on the Nafion®–silica nanocomposite membranes and the final loading amount of ink was 3 mg cm^{-2} for both electrodes. The catalyst-coated membrane was sandwiched between carbon papers (B-2/090/Stardard Wet Proofing Carbon Paper, Toray, Tokyo, Japan) and then hot-pressed at 130 °C under 80 kgf cm^{-2} for 3 min. The effective membrane area in the MEA was 5 cm^2 . The DMFC was operated at 90 °C with a feed rate of 1 mL min^{-1} of the methanol solution and 200 mL min^{-1} of oxygen at 0.1 MPa. Methanol concentrations of 1, 3, and 5 M were used to investigate the effect of methanol crossover on DMFC performance.

3. Results and discussion

3.1. Nafion®–silica nanocomposite membranes

The nomenclature of the Nafion®–silica nanocomposite membranes prepared in this study is provided in Table 2. A recast Nafion® membrane (Nafion® (recast)) was prepared as a control membrane for comparison with the Nafion®–silica nanocomposite membranes. For all Nafion®–silica nanocomposite membranes, 1 wt% hydrophobic surface-treated silica was used in this work. According to our previous results [23], a small amount of silica, if well dispersed within polymer electrolyte membranes, plays a significant role in improving DMFC performance via reduced methanol permeability without loss of proton conductivity. Therefore, in this study, the effect of silica content was not considered. In con-

trast to our previous study, however, hydrophobic surface-treated silica was employed instead of hydrophilic surface-treated silica because Nafion® consists of perfluorinated chains resulting in a predominantly hydrophobic nature; therefore it was predicted that hydrophobic silica would result in a better dispersed matrix than hydrophilic silica within the Nafion®. According to the manufacturer of the silica nanoparticles, the hydrophobicity of the silica used in this study is due to methyl groups on the silica surface.

Hereafter, Nafion®/silica refers to the Nafion®–silica nanocomposite membrane without any fluorosurfactant. Nafion®/silica/FS1 and Nafion®/silica/FS2 indicate nanocomposite membranes with fluorosurfactants (*i.e.*, Zonyl® FSP (FS1) and Zonyl® TBS (FS2)). Zonyl® FSP and Zonyl® TBS (*see Table 1*) are anionic-type fluorosurfactants because they have ionic end-groups such as phosphonic acid and sulfonic acid groups at the end of their fluorinated chains. These anionic-type fluorosurfactants are generally used in applications for which nonfluorinated surfactants are inadequate. In Nafion® membranes with an extremely hydrophobic nature, the surfactants may require extreme surface activity and chemical and thermal stabilities. In a preliminary study, it was found that hydrocarbon surfactants (*e.g.*, PEO_x–PPO_y–PEO_x triblock copolymer surfactant) are inappropriate as a dispersant for Nafion®–based nanocomposite membranes.

Generally, fluorosurfactants are more compatible than hydrocarbon surfactants in nearly all systems. Moreover, there is a significant difference in the surface tension of hydrocarbon surfactants and fluorosurfactants. Fluorosurfactants such as Zonyl® have surface tensions as low as 15 dyn cm^{-1} at 0.005 wt% in solution vs. 30 dyn cm^{-1} at 1 wt% in solution for typical hydrocarbon surfactants because of the strong electronegativity of fluorine relative to hydrogen [28]. It is well known that Zonyl® fluorosurfactants are far superior to nonfluorinated surfactants in terms of wetting action and both thermal and chemical stability in harsh environments. For ease of handling and dilution, most fluorosurfactants are formulated as liquids. In aqueous systems, half of the fluorosurfactant is hydrophilic and the other half is hydrophobic, which causes the surfactant to migrate to the interface where it can place its hydrophobic portion (fluorinated chains) into a non-aqueous phase such as an organic liquid or a hydrophobic surface in solid colloidal particles. In addition, hydrophobic surface-treated silica is easily mixed with Nafion® to reduce the methanol permeability through the composite membrane.

3.2. Thermal stability of Nafion®–silica nanocomposite membranes

To prepare Nafion® membranes recast from a Nafion® solution via a solution-casting method, heat treatment is required [29]. After heat treatment, the crystallinity of the recast Nafion® membrane increases, which helps improve the mechanical properties of the Nafion® membranes [29,30]. Therefore, the thermal stability of Nafion® membranes during heat treatment should be measured. The thermal stabilities of recast Nafion® and Nafion®–silica nanocomposite membranes are shown in Fig. 1. All membranes are stable up to around 250 °C in an oxidative air atmosphere. Nafion®/silica/FS1 and Nafion®/silica/FS2 begin to decompose at around 250 °C due to the degradation of fluorinated surfactants with lower molecular weights than Nafion®. Accordingly, the Nafion®–silica membranes containing fluorosurfactants were thermally heat-treated at temperatures below 250 °C.

3.3. Mechanical properties of Nafion®–silica nanocomposite membranes

The mechanical properties of polymer electrolyte membranes (PEMs) are a crucial determinant of the durability and safety of fuel

Table 2
Nomenclature of Nafion®–silica nanocomposite membranes.

Sample	Surfactant
Recast Nafion®	N/A
Nafion®/silica ^a	N/A
Nafion®/silica ^a /FS1	FS1 = Zonyl® FSP
Nafion®/silica ^a /FS2	FS2 = Zonyl® TBS

^a Silica = Aerosil 812 (hydrophobic surface-treated silica); silica loading content = 1 wt%.

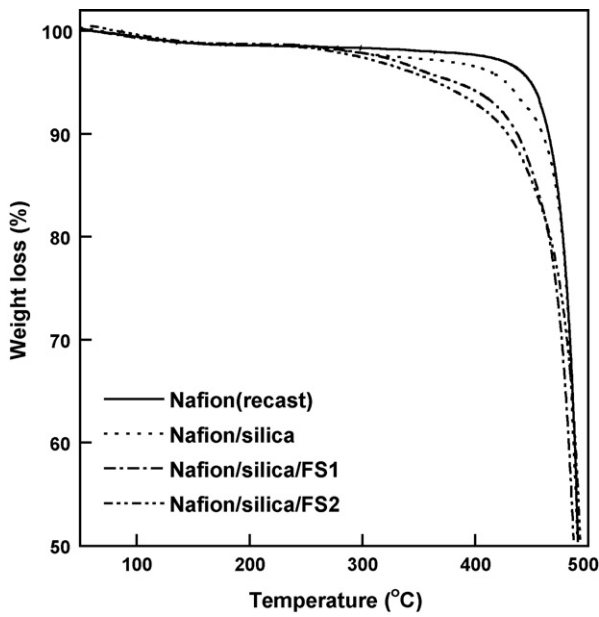


Fig. 1. Thermal stability of Nafion[®]-silica nanocomposite membranes in air.

cell systems. A high pressure of more than tens of kgf cm^{-2} is usually applied in the preparation of a membrane-electrode assembly (MEA). Polymer electrolyte membranes with lower mechanical stability can be easily broken or cracked. Moreover, the mechanical

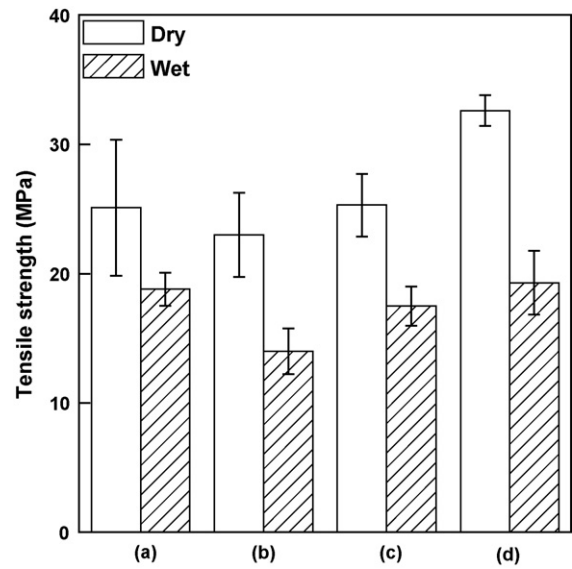


Fig. 2. Tensile strength (MPa) of Nafion[®]-silica nanocomposite membranes: (a) Nafion[®] (recast), (b) Nafion[®]/silica, (c) Nafion[®]/silica/FS1, and (d) Nafion[®]/silica/FS2.

properties of PEMs in the fully hydrated state should be carefully considered because the membranes are operated under humidified conditions. Fig. 2 shows the tensile strengths of Nafion[®]-silica nanocomposite membranes with and without fluorosurfactants, as well as that of the recast Nafion[®] membrane. The tensile strengths

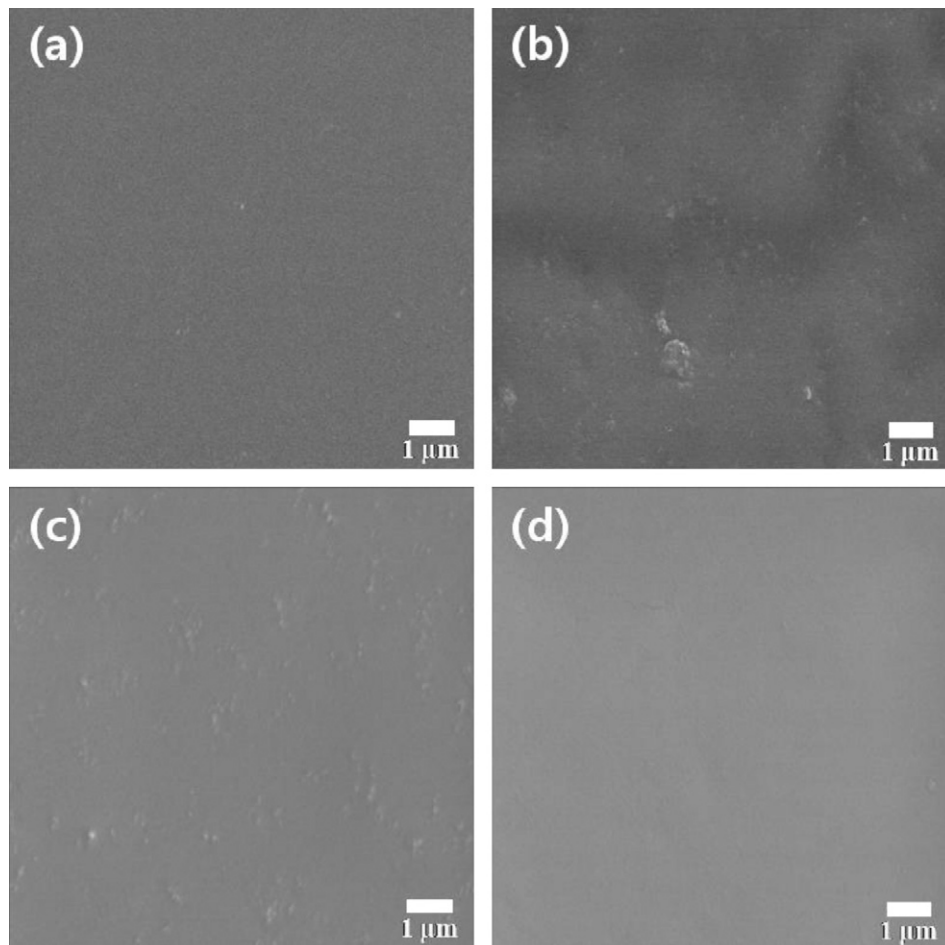


Fig. 3. Surface images of Nafion[®]-silica nanocomposite membranes: (a) Nafion[®] (recast), (b) Nafion[®]/silica, (c) Nafion[®]/silica/FS1, and (d) Nafion[®]/silica/FS2.

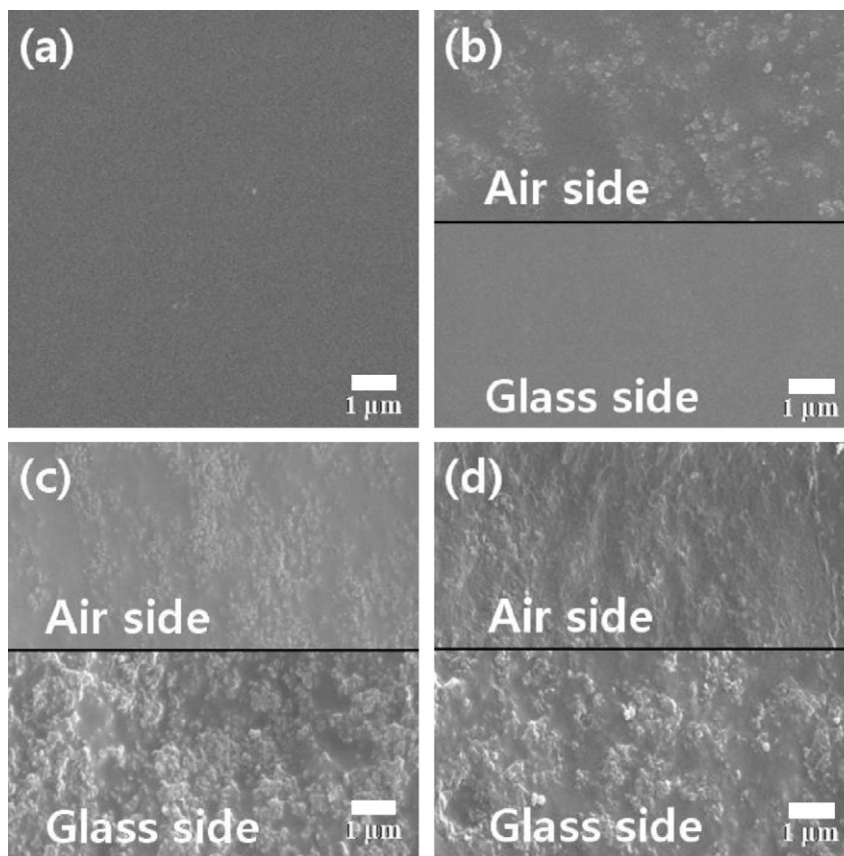


Fig. 4. Surface images (at air and glass sides) of Nafion[®]-silica nanocomposite membranes (3 wt% silica): (a) Nafion[®] (recast), (b) Nafion[®]/silica, (c) Nafion[®]/silica/FS1, and (d) Nafion[®]/silica/FS2.

of wet membranes are lower than those of dry membranes because of the low cohesive energy density between neighbouring chains due to absorbed water molecules in the hydrated state. In particular, addition of hydrophobic silica significantly decreases mechanical properties of the resulting nanocomposite membranes in the wet state due to the repulsion between hydrophobic silica and water molecules. Among the membranes tested, the Nafion[®]-silica membrane without any fluorosurfactant exhibited the lowest tensile strength, lower than that of the recast Nafion[®] membrane, particularly in the wet state. This indicates that the mechanical properties of nanocomposite membranes are negatively impacted by the addition of inorganic fillers that are not homogeneously distributed. When fluorosurfactants are added, however, the mechanical properties of nanocomposite membranes improve. This implies that the fluorosurfactants promote evenly distributed hydrophobic silica nanoparticles in the Nafion[®] membrane without the formation of large silica clusters due to self-agglomeration, and the amphiphilicity of the fluorosurfactants reduces the repulsion between hydrophobic silica and water molecules.

3.4. Dispersion of silica nanoparticles in Nafion[®] membranes

Fig. 3 shows scanning electron microscopy (SEM) images of the Nafion[®]-silica nanocomposite membranes. In Fig. 3, Nafion[®]/silica/FS1 and Nafion[®]/silica/FS2 membranes exhibit much smoother membrane surfaces than the Nafion[®]-silica membrane without fluorosurfactant. This indicates that the fluorosurfactants play a significant role in homogeneously distributing the silica nanoparticles. In particular, the membrane surface of Nafion[®]/silica/FS2 is very similar to that of the recast Nafion[®] membrane due to homogeneous distribution of silica nanoparticles that

results from the high compatibility of fluorosurfactant Zonyl[®] TBS with the Nafion[®] matrix by virtue of their structural similarity. This effect of the fluorosurfactants is clearly visible in the Nafion[®]-silica nanocomposite membranes containing 3 wt% silica (Fig. 4). Here, the Nafion[®]/silica membrane without surfactant has an asymmetric surface profile where silica is dispersed, which results from the

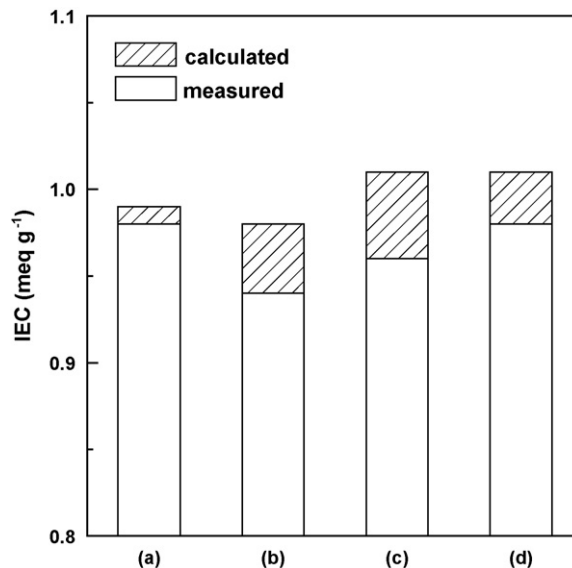


Fig. 5. Ion-exchange capacity (meq g⁻¹) values of Nafion[®]-silica nanocomposite membranes: (a) Nafion[®] (recast), (b) Nafion[®]/silica, (c) Nafion[®]/silica/FS1, and (d) Nafion[®]/silica/FS2.

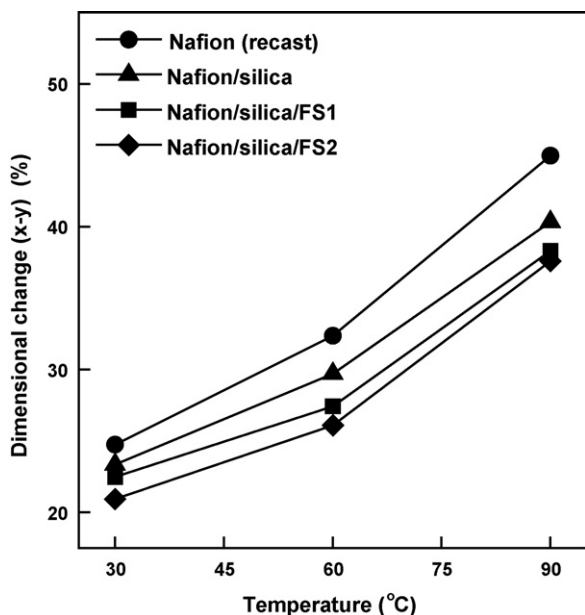


Fig. 6. Dimensional change (%) (x - y direction) of Nafion[®]-silica nanocomposite membranes as function of temperature.

lower density of silica compared with Nafion[®]. The orientation of hydrophobic silica to the air side, which is more hydrophobic than the glass plate, minimizes the interfacial free energy [31]. A significantly increased homogeneous dispersion of silica is obtained in the Nafion[®]/silica/FS1 and Nafion[®]/silica/FS2 membranes, irrespective of the air and glass sides of the membranes, and is due to the fluorosurfactants that stabilize hydrophobic silica within the Nafion[®] matrix.

3.5. IEC, water uptake, proton conductivity, and methanol permeability

The calculated and measured IEC values of the recast Nafion[®] and Nafion[®]-silica nanocomposite membranes are shown schematically in Fig. 5. In general, the IEC values increase with the amount of sulfonic acid groups, but decrease with the total polymer weight. The IEC value of the recast Nafion is 0.99 meq g^{-1} . The IEC values of the Nafion[®]-silica without fluorosurfactant are lower than that of recast Nafion[®] because of the increase of total weight due to the addition of silica nanoparticles without ionizable groups. The IEC values of Nafion[®]/silica/FS1 and Nafion[®]/silica/FS2 are higher than that of recast Nafion[®] because of the acidic functional groups in the fluorosurfactants, such as phosphonic and sulfonic acid groups, which exceed the effect of the increase of total weight of the Nafion[®]-silica nanocomposite membranes. By comparing the measured and calculated IEC values, the relative effects of additional acid groups and weight gain on the IEC values of Nafion[®]-silica nanocomposite membranes can be better understood. The theoretical and measured IEC values of the recast Nafion[®] membrane are not significantly different. By contrast, the measured IEC values of Nafion[®]/silica/FS1 and Nafion[®]/silica/FS2 are lower than the theoretical IEC values. For Nafion[®]/silica/FS2, this behaviour is due to the fact that the sulfonic acid group at the end of the fluorosurfactant chain has lower acidity than that at the end of the perfluorinated side chain in Nafion[®] owing to the absence of the inductive effect of the electron-withdrawing fluorine group [32]. As such, the Nafion[®]/silica/FS1 membrane has a lower measured IEC value than the Nafion[®]/silica/FS2 membrane due to the lower acidity of the phosphonic acid group in the Zonyl[®] FSP fluorosurfactant. In addition, this feature arises because

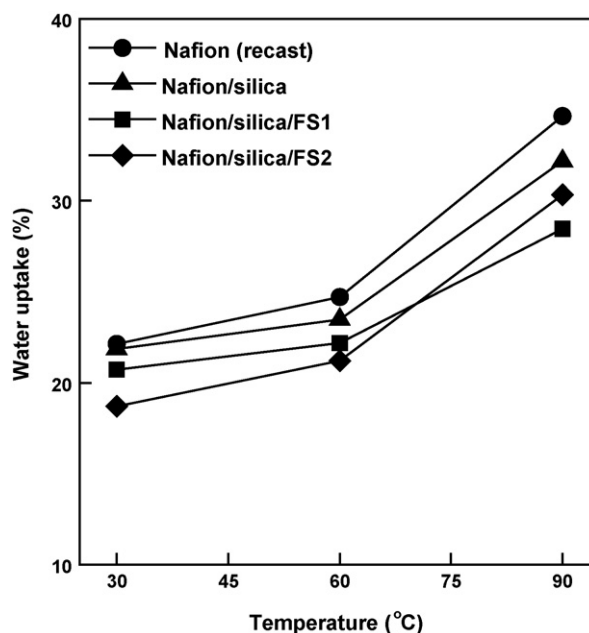


Fig. 7. Water uptake (%) of Nafion[®]-silica nanocomposite membranes as function of temperature.

both anionic fluorosurfactants also disperse into the hydrophobic regions of the Nafion[®]-silica nanocomposite membranes so that the acidic groups surrounded by hydrophobic segments cannot contribute to an increase in the IEC values of Nafion[®]/silica/FS1 and Nafion[®]/silica/FS2 [33]. For the Nafion[®]-silica membrane without fluorosurfactant, the measured IEC value is lower than the theoretical IEC value due to the effects of the total weight gain and reduced dispersion.

The effect of fluorosurfactant type on the dimensional change of Nafion[®]-silica nanocomposite membranes in the fully hydrated state is illustrated in Fig. 6. Water management in PEMs is a crucial issue for membrane durability and cell performance. During fuel cell operation, membranes cycle between dry and hydrated states, so that the membranes repeatedly swell and shrink. As a result, high dimensional changes in membranes due to high water uptake can lead to membrane failure, while insufficient water uptake results in reduced proton conduction, because proton transport occurs through hydrophilic water channels *via* the vehicle mechanism in the case of sulfonated polymer-based electrolyte membranes [34,35]. An attempt was made to control the water-swelling properties by incorporating hydrophobic silica. In Fig. 6, all Nafion[®]-silica nanocomposite membranes have less dimensional change than the recast Nafion[®] membrane because of their increased hydrophobicity due to the addition of hydrophobic silica. Furthermore, Nafion[®]-silica membranes with anionic fluorosurfactants have less dimensional change than membrane without fluorosurfactant despite the presence of acid groups that have an affinity for water molecules. This result can be explained by the homogeneous distribution of hydrophobic silica in the Nafion[®] membrane that is promoted by the fluorosurfactants. A comparison of Nafion[®]/silica/FS1 and Nafion[®]/silica/FS2 provides clear evidence of the relationship between water swelling properties and silica distribution. Nafion[®]/silica/FS2 with more homogeneous silica distribution, as discussed in Section 3.4, experience relatively low water swelling. Accordingly, well-dispersed hydrophobic silica can effectively increase the hydrophobicity of Nafion[®]-silica nanocomposite membranes. The water uptake results in Fig. 7 show similar trends to the dimensional change in the x - y direction.

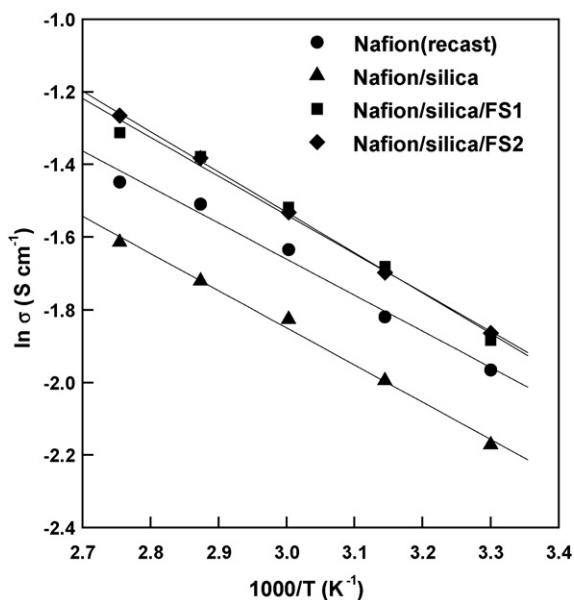


Fig. 8. Proton conductivity of Nafion[®]-silica nanocomposite membranes as function of temperature.

Proton conductivity is a key factor that determines fuel cell performance, and is strongly affected by IEC values, water uptake, and the distribution of ionic groups such as sulfonic acid. As shown in Fig. 8, the Nafion[®]-silica nanocomposite membrane without fluorosurfactant shows lower proton conductivity than the recast Nafion[®] membrane due to its relatively low IEC value caused by the addition of non-conductive hydrophobic silica. By contrast, the proton conductivities of Nafion[®]/silica/FS1 and Nafion[®]/silica/FS2 are higher than that of the recast Nafion[®] membrane despite slightly lower or similar IEC values, respectively. This may be due to the homogeneous distribution of anionic fluorosurfactant with silica nanoparticles throughout the Nafion[®] matrix. In PEMs, two proton conduction mechanisms have been proposed: the Grotthuss and vehicle mechanisms [36]. In the Grotthuss mechanism, proton transport can be achieved *via* a hopping mechanism by the making and breaking of hydrogen bonds [36,37]. That is, additional acid groups in anionic fluorosurfactants can contribute to the formation of more hydrogen bonds, leading to higher proton conductivity. Moreover, at the same IEC value, lower water swelling of Nafion[®]/silica/FS1 and Nafion[®]/silica/FS2 membranes compared with the recast Nafion[®] membrane can improve proton conductivity. If two PEMs have the same IEC value (the mole equivalent of sulfonic acid groups per gram of polymer), they have the same amount of sulfonic acid groups. In the water swollen state, however, the concentration of sulfonic acid groups in a PEM decreases because of the absorbed water molecules, so that a PEM with lower water uptake can allow higher proton conduction at the same IEC value than a PEM with higher water uptake [38].

As mentioned previously, fuel leaks (*i.e.*, methanol crossover) are a major problem in current DMFC systems, and these can be influenced by the microstructure of the hydrophilic channels. As shown in Fig. 9, all Nafion[®]-silica nanocomposite membranes, irrespective of the presence of fluorosurfactants, have lower methanol permeability than the recast Nafion[®] membrane due to the addition of an inorganic hydrophobic silica nanoparticle filler. Moreover, Nafion[®]-silica nanocomposite membranes with fluorosurfactants have lower methanol permeability than nanocomposite membranes without fluorosurfactant. In general, the methanol permeability of the membrane has a strong relationship with the dimensional stability of the membrane, because the total amount

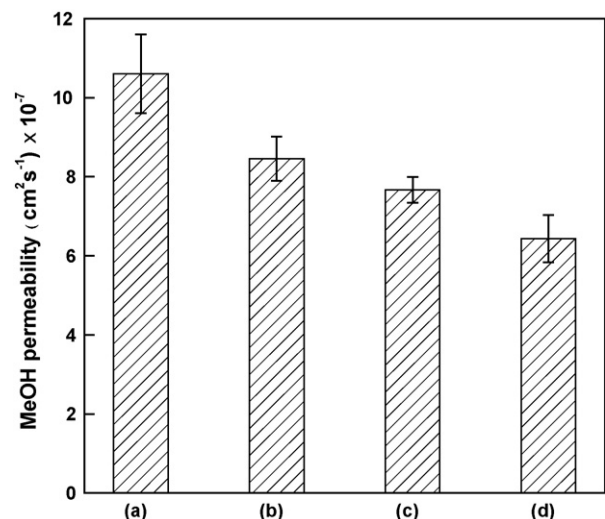


Fig. 9. Methanol permeability of Nafion[®]-silica nanocomposite membranes at 25 °C: (a) Nafion[®] (recast), (b) Nafion[®]/silica, (c) Nafion[®]/silica/FS1, and (d) Nafion[®]/silica/FS2.

of permeates is proportional to the area of the membrane, which swells with the water and methanol mixture in DMFC. That is, higher water swelling usually leads to higher methanol permeability. Consequently, Nafion[®]/silica/FS2 has a lower methanol permeability than Nafion[®]/silica/FS1 according to their dimensional stability data.

3.6. Cell performance of Nafion[®]-silica membranes

Membrane-electrode assemblies (MEAs) were prepared using Nafion[®]-silica nanocomposite membranes for a single-cell test in DMFC. The cell performance is affected by various membrane properties such as IEC, proton conductivity, methanol permeability, and water uptake. In this study, polarization curves were measured using an electronic loader at three different methanol concentrations (1, 3, and 5 M) to study the effect of methanol permeability of Nafion[®]-silica nanocomposite membranes. The single-cell performance of the nanocomposite membranes with various fluorosurfactants is presented in Fig. 10. The performance of a single-cell test with a Nafion[®] 117-based MEA was also evaluated for comparison. In this work, the current density at 0.4 V and the maximum (max) power density are used as indices of single-cell performance.

As shown in Fig. 10a (1 M methanol), the cell performance is strongly affected by the methanol barrier properties of the Nafion[®]-silica nanocomposite membranes. As discussed above, Nafion[®]/silica/FS2 has the lowest methanol permeability and the highest proton conductivity, which leads to the best electrochemical performance of 342 mA cm⁻² (current density) at 0.4 V and 138 mW cm⁻² (maximum power density). The current density and maximum power density of the recast Nafion[®] membrane are 254 mA cm⁻² at 0.4 V and 103 mW cm⁻², respectively.

A high methanol concentration at the anode side can lead to high methanol permeation through the PEM, which causes a drastic fall in cell performance in the low current density region as well as a low open-circuit voltage (OCV). On the other hands, enriched fuel conditions can decrease concentration polarization in the high current region where fuel consumption occurs quickly. As the methanol concentration is increased to 3 M (Fig. 10b), the cell performance (current density at 0.4 V and maximum power density) of all membranes is enhanced, although the OCVs with the 3 M methanol solution are lower than those with the 1 M methanol solution due

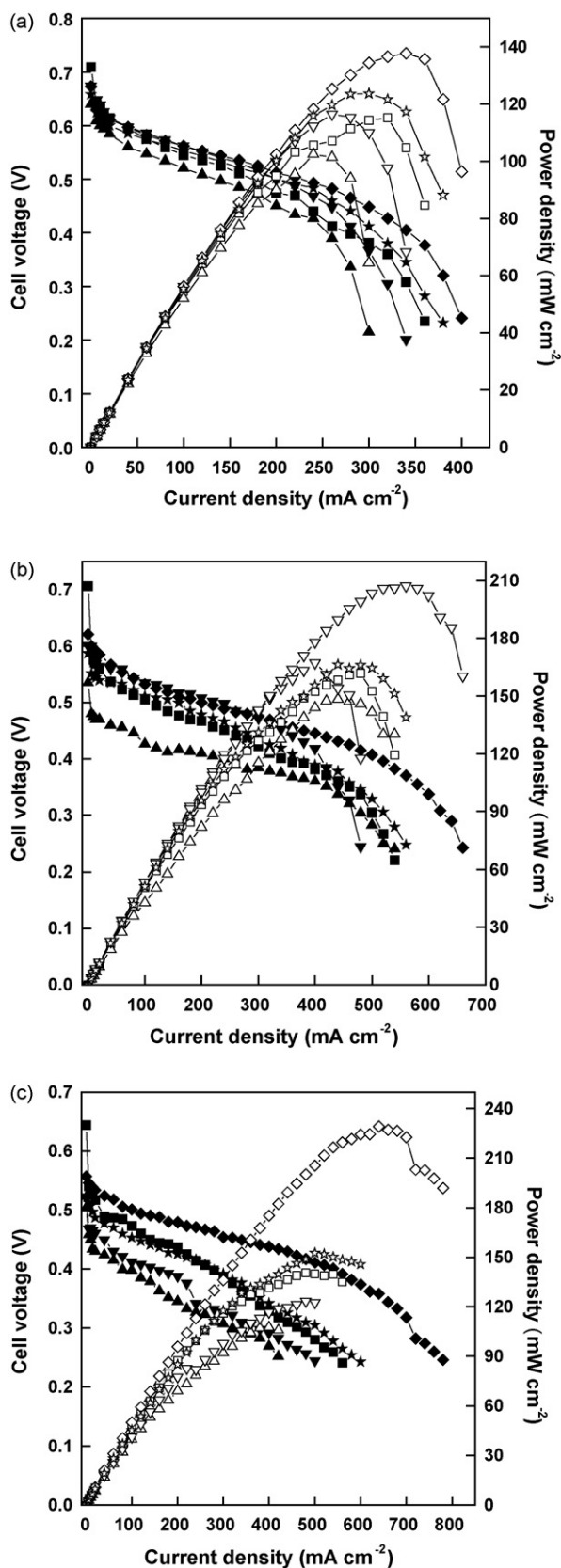


Fig. 10. V - I and P - I curves of DMFC with different MEAs prepared from Nafion[®] 117 (control) (■), Nafion[®] (recast) (▲), Nafion[®]/silica (▼), Nafion[®]/silica/FS1 (*), and Nafion[®]/silica/FS2 (◆). Fuel cell run at 90 °C with anode fed with (a) 1, (b) 3 and (c) 5 M CH₃OH at 1 mL min⁻¹ and cathode fed with O₂ at 0.1 MPa and 200 mL min⁻¹.

to increased methanol crossover. Nafion[®]-silica nanocomposite membranes without fluorosurfactant exhibit somewhat unstable polarization curves and poorer cell performances compared with Nafion[®]-silica nanocomposite membranes with fluorosurfactants, because the lower have a lower proton conductivity in the hydrated state.

When the methanol concentration is increased to 5 M, the effect of increased methanol crossover on cell performance becomes larger than that of reduced concentration polarization, as shown in Fig. 10c. As a result, all membranes tested in this work, except for the Nafion[®]/silica/FS2 membrane, exhibit significant drops in their polarization curves at the low current density and thus decreased cell performances compared with their performance in the 3 M methanol solution. Nevertheless, the Nafion[®]/silica/FS2 membrane still shows the highest cell performance of 538 mA cm⁻² (current density) at 0.4 V and 229 mW cm⁻² (maximum power density) in the 5 M methanol solution due to the fact that it has the lowest methanol permeability as well as highest proton conductivity.

4. Conclusions

To improve the performance of DMFCs, Nafion[®]-silica nanocomposite membranes have been prepared using fluorosurfactants, which promote the homogeneous dispersion of silica nanoparticles in the Nafion[®] matrix. The enhanced performance of MEAs prepared from such Nafion[®]-silica nanocomposite membranes is verified through DMFC experiments. The MEAs show an increase in peak output power density compared with MEAs with Nafion[®] and Nafion[®]-silica nanocomposite membranes without any fluorosurfactants. The fluorosurfactants contribute to both homogeneous silica dispersion and improved cell performance. That is, well-dispersed hydrophobic silica is observed in Nafion[®]-silica nanocomposite membranes with fluorosurfactants, which result in an improvement in the mechanical stability of the membrane and a reduction in water swelling. Low methanol crossover is also achieved as a result of low water uptake. In addition, ionic groups of fluorosurfactants such as phosphonic and sulfonic acid groups lead to increased IEC values and proton conductivities. In particular, the Nafion[®]-silica composite membrane with Zonyl[®] TBS fluorosurfactant shows the best result in terms of dispersion properties and IEC, proton conductivity and methanol permeability. This is because the Zonyl[®] TBS fluorosurfactant has a similar chain structure to the Nafion[®] matrix. As a result, the Nafion[®]-silica nanocomposite membrane with Zonyl[®] TBS gives better DMFC performance than the commercial Nafion[®] 117 membrane and the recast Nafion[®] membrane. The DMFC performance data of the Nafion[®]-silica nanocomposite membrane with Zonyl[®] TBS are markedly better than those of all the other membranes at a higher methanol concentration because of the very low methanol permeability of the Nafion[®]-silica nanocomposite membrane with Zonyl[®] TBS.

Acknowledgements

This work was supported by the Korean Foundation for International Cooperation of Science & Technology (KICOS) through a grant provided by the Korean Ministry of Education, Science & Technology (K20701010356-07A0100-10610). C.H. Park and H.K. Kim wish to express their gratitude to the BK21 Project for their fellowships.

References

- [1] A.J. Appleby, F.R. Foulkes, Fuel Cell Handbook, Van Nostrand Reinhold, New York, 1989.
- [2] O. Savadogo, J. New Mater. Electrochem. Syst. 1 (1998) 47.

- [3] B.C.H. Steele, A. Heinzel, *Nature* 414 (2001) 345.
- [4] A.S. Arico, S. Srinivasan, V. Antonucci, *Fuel Cells* 1 (2001) 133.
- [5] W.M. Yang, S.K. Chou, C. Shu, *J. Power Sources* 164 (2007) 549.
- [6] Y. Nishi, *J. Power Sources* 100 (2001) 101.
- [7] Y. Muranaka, A. Ueda, T. Nishida, K. Soma, *Hitachi Rev.* 55 (2006) 40.
- [8] K. Scott, W.M. Taama, P. Argyropoulos, K. Sundmacher, *J. Power Sources* 83 (1999) 204.
- [9] C.H. Rhee, H.K. Kim, H. Chang, J.S. Lee, *Chem. Mater.* 17 (2005) 1691.
- [10] B. Smitha, S. Sridhar, A.A. Khan, *Macromolecules* 37 (2004) 2233.
- [11] D.S. Kim, H.B. Park, J.W. Rhim, Y.M. Lee, *Solid State Ionics* 176 (2005) 117.
- [12] H.B. Park, C.H. Lee, J.Y. Sohn, Y.M. Lee, B.D. Freeman, H.J. Kim, *J. Membr. Sci.* 285 (2006) 432.
- [13] H.L. Tang, M. Pan, S.P. Jiang, R.Z. Yuan, *Mater. Lett.* 59 (2005) 3766.
- [14] J. Won, H.H. Park, Y.J. Kim, S.W. Choi, H.Y. Ha, I.-H. Oh, H.S. Kim, Y.S. Kang, K.J. Ihn, *Macromolecules* 36 (2003) 3228.
- [15] S. Zhong, X. Cui, T. Fu, H. Na, *J. Power Sources* 180 (2008) 23.
- [16] Z. Chen, B. Holmberg, W. Li, X. Wang, W. Deng, R. Munoz, Y.S. Yan, *Chem. Mater.* 18 (2006) 5669.
- [17] A. Saxena, B.P. Tripathi, V.K. Shahi, *J. Phys. Chem. B* 111 (2007) 12454.
- [18] W. Lee, H. Kim, T.K. Kim, H. Chang, *J. Membr. Sci.* 292 (2007) 29.
- [19] R. Jiang, H.R. Kunz, J.M. Fenton, *J. Membr. Sci.* 272 (2006) 116.
- [20] D.S. Kim, H.B. Park, J.W. Rhim, Y.M. Lee, *J. Membr. Sci.* 240 (2004) 37.
- [21] J.Y. Kim, S. Mulmi, C.H. Lee, H.B. Park, Y.S. Chung, Y.M. Lee, *J. Membr. Sci.* 283 (2006) 172.
- [22] C.H. Lee, S.Y. Hwang, J.Y. Sohn, H.B. Park, J.Y. Kim, Y.M. Lee, *J. Power Sources* 163 (2006) 339.
- [23] C.H. Lee, K.A. Min, H.B. Park, Y.T. Hong, B.O. Jung, Y.M. Lee, *J. Membr. Sci.* 303 (2007) 258.
- [24] K.T. Adjemian, R. Dominey, L. Krishnan, H. Ota, P. Majsztrik, T. Zhang, J. Mann, B. Kirby, L. Gatto, M. Velo-Simpson, J. Leahy, S. Srinivasan, J.B. Benziger, A.B. Bocarsly, *Chem. Mater.* 18 (2006) 2238.
- [25] G. Ye, C.A. Hayden, G.R. Goward, *Macromolecules* 40 (2007) 1529.
- [26] Z. Qi, A. Kaufman, *J. Power Sources* 110 (2002) 177.
- [27] C.H. Lee, H.B. Park, Y.M. Lee, R.D. Lee, *Ind. Eng. Chem. Res.* 44 (2005) 7617.
- [28] E. Kissa, *Fluorinated Surfactants and Repellents*, CRC Press, Boca Raton, 2001.
- [29] K.A. Mauritz, R.B. Moore, *Chem. Rev.* 104 (2004) 4535.
- [30] H.-Y. Jung, K.-Y. Cho, Y.M. Lee, J.-K. Park, J.-H. Choi, Y.-E. Sung, *J. Power Sources* 163 (2007) 952.
- [31] H. Ni, H. Zhang, X. Wang, X. Wang, *J. Appl. Polym. Sci.* 106 (2007) 3975.
- [32] J.M. Hornback, *Organic Chemistry*, Thomson Brooks/Cole, Belmont, 2005.
- [33] T.Y. Chen, J. Leddy, *Langmuir* 16 (2000) 2866.
- [34] K.D. Kreuer, S.J. Paddison, E. Spohr, M. Schuster, *Chem. Rev.* 104 (2004) 4637.
- [35] J. Fimrite, H. Struchtrup, N. Djilali, *J. Electrochem. Soc.* 152 (2005) A1804.
- [36] K.D. Kreuer, *Chem. Mater.* 8 (1996) 610.
- [37] D.S. Kim, B. Liu, M.D. Guiver, *Polymer* 47 (2006) 7871.
- [38] Y.S. Kim, D.S. Kim, B. Liu, M.D. Guiver, B.S. Pivovar, *J. Electrochem. Soc.* 155 (2008) B21.